JOURNAL OF MATERIALS SCIENCE **38** (2003) 1793–1802

Effect of interfacial interaction on morphology and mechanical properties of PP/POE/$BaSO_4$ ternary composites

ZHEN LI
The State Key Laboratory of Polymer Materials Engineering, Polymer Research Institute of Sichuan University, Chengdu 610065, People's Republic of China; Resin Research Institute of Qilu Petrochemical Co. SINOPEC, Zibo 255400, People's Republic of China

SHAOYUN GUO*
The State Key Laboratory of Polymer Materials Engineering, Polymer Research Institute of Sichuan University, Chengdu 610065, People's Republic of China
E-mail: nic7702@pridns.scu.edu.cn

WENTAO SONG, BIN HOU
Resin Research Institute of Qilu Petrochemical Co. SINOPEC, Zibo 255400, People's Republic of China

Ternary composites of Polypropylene (PP)/ethylene-octene copolymer (POE)/Barium Sulfate ($BaSO_4$) (PP/POE/$BaSO_4$) were prepared through a two-step process: $BaSO_4$ master-batches were first prepared through blending of $BaSO_4$ and POE, then blending with PP. Two families of phase structure were confirmed through SEM and DSC, depending on their interfacial interaction. Separation of POE and $BaSO_4$ filler was found when untreated or titanate coupling agent treated $BaSO_4$ filler were used. Encapsulation of $BaSO_4$ particles by POE elastomer was achieved by using $BaSO_4$ master-batch prepared through reactive blending of $BaSO_4$ with POE in the presence of maleic anhydride (MAH) and dicumyl peroxide (DCP). The mechanical properties of the composites greatly rely on the morphology. The yield strength and the impact toughness of a composite with core-shell morphology are higher than those of composites with separated morphologies, but the former has lower flexural modulus and elongation at break than the latter. The interfacial interaction was evaluated by semi-empirical equations developed previously. The deformation and toughening mechanisms of the composites were also investigated.

1. Introduction

In addition to reduce cost, fillers are also used to modify the physical properties of polypropylene, such as flexural modulus and heat distortion temperature, or to endow some special functions e.g., flame retardancy and magnetic properties. Although some results indicate an increase in toughness with rigid particle fillers in certain filled PP systems [1, 2], most of the studies of filled PP report a significant decrease of toughness compared with unfilled PP, especially at high filler loadings. On the other hand, elastomers can effectively improve the low temperature toughness of PP, but significantly decrease its stiffness. In view of the above situations, PP/elastomer/filler ternary composites have become attractive materials for numerous engineering applications due to their potentially high stiffness and high toughness. The mechanical properties of such composites are determined not only by composition, but also by the morphology present, especially the relative spatial arrangement of elastomer and filler inclusions [3, 4], which depends strongly on mixing conditions, the rheology and surface energies of the components and the geometry of the rigid fillers.

Mutual miscibility and adhesion of the constituents are the crucial factors influencing the structure and the property relationships in ternary composites [5]. Two families of morphologies are assumed in PP ternary composites: (i) elastomer and filler particles are separately dispersed in PP matrix; (ii) elastomer encapsulates filler particles to form core-shell inclusions [3, 5–9]. The morphological structure was controlled by the interfacial adhesion of PP-filler and elastomer-filler. Recently, functionalized polymers are introduced into PP ternary composites to adjust the interfacial adhesion [10–12]. When adhesion between PP matrix and rigid filler is enhanced by the addition of maleic anhydride

*Author to whom all correspondence should be addressed.

grafted PP, the elastomer and the rigid filler are separately dispersed in PP matrix, whereas when adhesion between the elastomer phase and rigid filler is enhanced by the incorporation of maleic anhydride grafted elastomer or other polar elastomers, the filler becomes encapsulated by the elastomer, promoting the formation of core-shell inclusions [10–12]. These two different morphologies gave significantly distinct mechanical properties. Ternary composites with separated structure have been reported to have higher modulus and yield strength than those containing encapsulated filler, whereas the latter exhibited higher impact strength [3, 13, 14].

The aim of the present work was to study the effect of interfacial interaction on the morphology and mechanical properties of PP/POE/$BaSO_4$ ternary composites. The preparation of ternary composites was through a two-step process, in which three kinds of $BaSO_4$ master-batches with different interfacial interaction were prepared first, and then blended with PP matrix. Reactive extrusion was used to prepare $BaSO_4$ master-batch, where the surface treatment of $BaSO_4$ filler and the functionalization of POE elastomer with maleic anhydride were performed in situ in the presence of peroxide. The morphology of thus formed the ternary composite was analyzed using SEM and compared with those of two other kinds of filled PP with $BaSO_4$ fillers (untreated and titanate coupling agent treated). Emphasis is given to analyzing the effect of morphology and interfacial interaction on the crystallization of the PP matrix and the mechanical properties of the composites. In view of the results of SEM observation, the toughening mechanisms of ternary composites are proposed.

2. Experimental

2.1. Materials

PP matrix used in this study was a block copolymer (EPS30R) with 8.5 wt% ethylene comonomer from Qilu Petrochemical Co. SINOPEC, China with a melt flow index of 2.0 g/10 min and a density of 0.9 g/cm^3. Elastomer used was ethylene-octene copolymer (POE) EG8150 from Dupont Dow Elastomer Co. with a octene content of 25 wt%, a nominal Mooney viscosity ML $(1+4)121^\circ$C of 35 and a density of 0.87 g/cm^3. $BaSO_4$ used was precipitated $BaSO_4$ produced by Jianghu Industry Co., China with a weight average diameter of 4.5 μm, polydispersity of 3.5, and a density of 4.4 g/cm^3. Maleic anhydride (MAH) and dicumyl peroxide (DCP) were used as grafting monomer and initiator respectively. The coupling agent used was isopropyl tri(dioctyl pyrophosphato) titanate NDZ-201 from Nanjing Chemical Factory No. 1, China.

2.2. Sample preparation

To ensure good dispersion of $BaSO_4$ filler, PP/POE/$BaSO_4$ ternary composites were prepared through a two-step process. Three kinds of $BaSO_4$ master-batches (Table I) containing 20 wt% POE elastomer and 80 wt% different surface treated $BaSO_4$ were first prepared in a co-rotating twin screw extruder with a diameter of 25 mm and L/D ratio of 30, then melt blended with PP matrix in the same extruder. The extrusion temperatures set at different zones from hopper to die were 160°C, 180°C, 190°C, and 200°C respectively. The screw speed was 200 rpm. The sample codes of the master-batches and their corresponding surface treatment of $BaSO_4$ are listed in Table I. As references, PP/POE binary blends with the same POE volume fraction as those in ternary composites were prepared using the same twin-screw extruder and extrusion conditions mentioned above.

TABLE I Sample code & treating ways of $BaSO_4$ master-batch

Sample code	Carrier resin	Pretreatment of filler
BM-0	POE	Untreated
BM-N	POE	Coupling agent of organic titanate
BM-M	POE	Maleic anhydride DCP

The test specimens for stress-strain behaviour, 3-point flexure and impact fracture behavior were prepared by injection moulding according to ASTM D638, ASTM D790, and ASTM D256 standard methods respectively. The injection temperatures from hopper to nozzle are 190°C, 200°C, 210°C and 210°C respectively, and the mould temperature is 40°C. Before injection, the granules of the composites were dried in a vacuum oven at 90°C for a period of 12 hr.

2.3. Measurements and characterization

Tensile tests were made using an Instron 4302 tensile testing machine at a crosshead speed of 50 mm/min in accordance with ASTM D638 standard method. The 3-point flexure tests were performed using an Instron 4302 tensile testing machine at a crosshead speed of 2 mm/min according to ASTM D 790 standard method. Notched Izod impact tests were conducted on a CEAST impact tester with an impact velocity of 3.46 m/s according to ASTM D256. All tests were carried out at 23°C.

DSC analysis was conducted with a Dupont 2100 DSC instrument. The test specimens (5–10 mg) were first heated from 30 to 200°C at a rate of 10°C/min and maintained at 200°C for a period of 5 min, then cooled down to 30°C at the same rate, after that heated again from 30°C to 200°C with a rate of 10°C/min. Melting and crystallization thermograms were recorded, and thus crystallization temperature T_c, and melting temperature T_m, were obtained.

The phase structure and fractured behavior of the ternary composites were examined by scanning electron microscope (SEM) analysis. For phase structure observation, fractured surfaces of the composites under liquid nitrogen temperature were etched for a period of 5 min in boiling n-heptane to remove POE, then coated with silver-palladium alloy and examined with a HITACHI X-650 SEM instrument with an accelerating voltage of 20 kv. For fractured behavior analysis, the tensile fractured surfaces were cut open parallel to tensile direction under liquid nitrogen temperature. The impact fractured surfaces and longitudinal open

sections were coated with silver-palladium alloy and examined with a HITACHI X-650 SEM instrument with an accelerating voltage of 20 kv.

3. Results and discussion

3.1. Morphology

SEM micrographs of the etched cryogenic fracture surfaces of PP/POE/$BaSO_4$ ternary composites are shown in Fig. 1. The dark holes represent POE elastomer droplets, which are dissolved out by selective etching, whereas the brighter irregular shape particles are $BaSO_4$ filler. SEM micrographs reveal separate dispersion of POE and $BaSO_4$ particles in PP matrix for ternary composites containing untreated $BaSO_4$ filler (Fig. 1a) and titanate coupling agent treated $BaSO_4$ filler (Fig. 1b). A contrary morphology is shown in Fig. 1c for ternary composites containing $BaSO_4$ master-batch prepared through reactive extrusion in the presence of MAH and DCP. Fig. 1c indicates that in the ternary composite containing $BaSO_4$ master-batch prepared through reactive extrusion in the presence of MAH and DCP, MAH functionalized POE could encapsulate $BaSO_4$ particles due to the strong interaction of MAH group with $BaSO_4$, forming core-shell inclusion structure. The etched POE elastomer was observed as voids around the filler particles. As shown by previous studies on PP ternary composites [3, 8], a complete encapsulation was also achieved by using functionalized elastomer.

DSC studies of non-isothermal crystallization and melting behavior were performed in order to investigate the influence of phase morphology on the crystallization of PP in the blends, which were also used as an indirect method for verifying the phase structure of ternary composites. Table II shows the T_c, $T_{c(onset)}$, and T_m of PP composites at various compositions. These data demonstrate that POE and $BaSO_4$ have slight influence on the T_m of PP. In PP/POE and PP/$BaSO_4$ binary systems, the incorporation of POE induces a very slight increase of T_c and $T_{c(onset)}$ of PP, which was also found in previous studies of PP/elastomer systems [15–18],

TABLE II DSC crystallization and melting data of PP/POE/$BaSO_4$

	Weight ratio	Crystallization		Melting
		$T_{c(onset)}$ (°C)	T_c (°C)	T_m (°C)
PP	100/0/0	114.7	111.7	161.4
PP/POE	89.3/10.7/0	115.1	111.8	161.6
PP/$BaSO_4$	60/0/40	121.6	116.9	161.9
PP/BM-0	60/8/32	119.9	117.5	162.1
PP/BM-N	60/8/32	118.3	115.5	161.4
PP/BM-M	60/8/32	115.6	113.5	161.1

indicating that POE has very weak influence on the kinetics of crystallization of PP. While the presence of $BaSO_4$ significantly increases the T_c and $T_{c(onset)}$ of PP and decreases degree of super cooling ΔT, indicating that $BaSO_4$ greatly promotes the crystallization of PP by acting as a nucleating agent. The results show that as compared with unfilled PP, if PP in the ternary composites has much higher T_c and $T_{c(onset)}$, the composites should have a separate morphology in which POE and $BaSO_4$ particles are separately dispersed in PP matrix, and vice versa. Therefore the phase morphology of the ternary composites could be confirmed by the measurement of T_c and $T_{c(onset)}$ of PP in ternary composites.

For ternary composites containing BM-M master-batch, no influence of $BaSO_4$ on the T_c and $T_{c(onset)}$ values of PP was observed. Both values remain unchanged with the increasing of POE elastomer and $BaSO_4$ filler. The reduction in nucleating efficiency of $BaSO_4$ filler in the PP/BM-M system is therefore a result of the encapsulation of $BaSO_4$ particles by the POE elastomer. Contrary results were observed for PP/BM-0 and PP/BM-N systems, in which the T_c and $T_{c(onset)}$ values of PP were found to increase as the contents of both $BaSO_4$ and POE elastomer increased. This observation implied a direct contact of $BaSO_4$ to the PP matrix, demonstrating a separate dispersion of $BaSO_4$ filler and POE elastomer in PP matrix. In addition, a small difference exists in T_c and $T_{c(onset)}$ values in these two systems. A reduction in T_c and $T_{c(onset)}$ values were observed for ternary composite containing titanate coupling agent treated $BaSO_4$ filler as compared with composite containing untreated

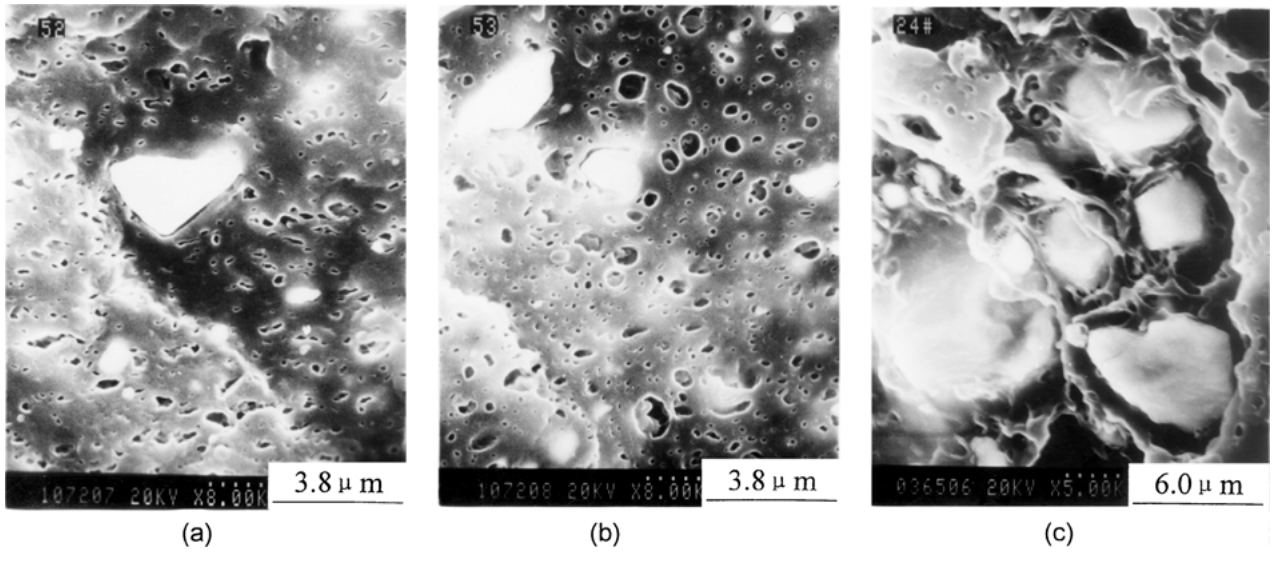

Figure 1 SEM micrographs of fractured and etched surfaces of PP/POE/$BaSO_4$ (60/8/32) composites: (a) PP/BM-0, (b) PP/BM-N, and (c) PP/BM-M.

filler particles. This may be attributed to the decrease of PP matrix-filler interaction in the presence of coupling agent, because the adsorption of large molecules on the surface of a foreign phase is influenced by the interaction between them, and is very crucial for the heterogeneous nucleation during crystallization [19]. DSC results are consistent with SEM observation.

3.2. Mechanical properties

As shown in Fig. 2, the incorporation of POE elastomer to PP decreased the yield stress of PP/POE binary composites, which is a result of poor interfacial adhesion between matrix and elastomer [20]. The decrease in yield stress became more pronounced when $BaSO_4$ filler was incorporated into the PP/POE composites. In PP/BM-0 ternary composites, all interfaces (i.e., PP/POE, PP/$BaSO_4$ and POE/$BaSO_4$) are too weak to sustain stress transfer between phases due to poor interfacial adhesion, the effects of filler and elastomer on the yield stress are reported to have approximate additivity [21]. The addition of titanate coupling agent treated $BaSO_4$ filler decreases the yield stress even further. The contrary results were observed for PP/BM-M composites. As the volume fraction of BM-M master-batch (i.e., both the $BaSO_4$ filler and the elastomer volume fraction) increased, the yield stress decreased a little, and then increased. The increase in yield stress may be attributed to the improved adhesion between the $BaSO_4$ filler core and the POE elastomer shell, owing to the presence of covalent bond or specific interaction formed by the in situ modification of $BaSO_4$ filler and the functionalization of POE with maleic anhydride during the preparation of BM-M master-batch.

Changes in interfacial interactions can modify the mechanism of micro-mechanical deformation, failure behaviour, and thus the overall performance of composite, therefore can provide useful information for preparing tailor-made composites. Yield stress proved to be an excellent property to predict interfacial interaction quantitatively in heterogeneous polymer systems. A model developed previously [22–25] described the effect of decreasing loadbearing cross-section areas and the interfacial interaction on the yield stress of particulate filled polymeric system. The expression of yield stress takes the form

$$\sigma_y = \sigma_{ym} \frac{1 - \varphi_f}{1 + 2.5\varphi_f} \exp(B_{\sigma y}\varphi_f) \tag{1}$$

where σ_y and σ_{ym} are the yield stresses of the composite and the matrix, respectively, φ_f is the volume fraction of the filler in the composite, and $B_{\sigma y}$ is the parameter characterizing interfacial interaction. The term $(1 - \varphi_f)/(1 + 2.5\varphi_f)$ takes into account the decrease of the effective load-bearing cross-section areas owing to the introduction of the filler into the matrix.

To evaluate the interfacial interactions in ternary composites studied here, PP/POE blend was assumed as matrix with the properties of the corresponding PP/POE binary blends. Equation 1 could be rearranged as

$$\ln\left[\frac{\sigma_y}{\sigma_{ym}} \frac{1 + 2.5\varphi_f}{1 - \varphi_f}\right] = B_{\sigma y}\varphi_f \tag{2}$$

According to Equation 2, the parameter $B_{\sigma y}$ was obtained and used for evaluating interfacial interaction quantitatively. As was show in Table III, interaction in PP/BM-M system is the strongest, whereas interaction in PP/BM-N system is the weakest due to the coupling agent softening PP matrix around filler particles.

Elongation at break of PP/BM-M system (with core-shell structure) is lower than those of the separated microstructures (PP/BM-O and PP/BM-N systems), and decreases with the increasing in volume fraction of $BaSO_4$ master-batch (Fig. 3). This finding is different from previous study on the elongation of ternary composite with core-shell structure [14]. It is well known that the incorporation of filler particles usually decreases the elongation at break of filled polymer system due to the intrinsic stiffness of the filler, whereas elastomer increases elongation at break of polymer blends

TABLE III $B_{\sigma y}$ values of PP ternary composites

Sample code	$B_{\sigma y}$
PP/BM-0	2.142
PP/BM-N	1.209
PP/BM-M	3.891

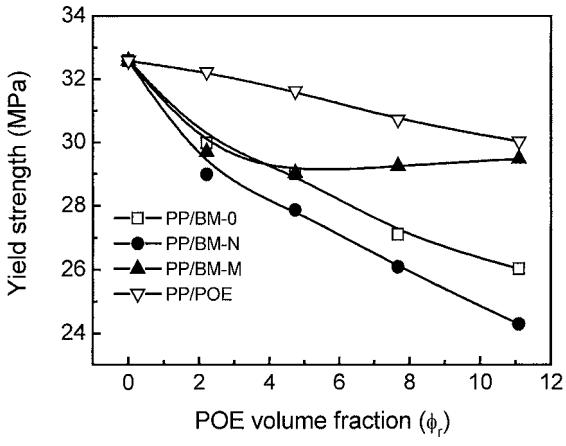

Figure 2 Yield strength vs. POE volume fraction in PP composites.

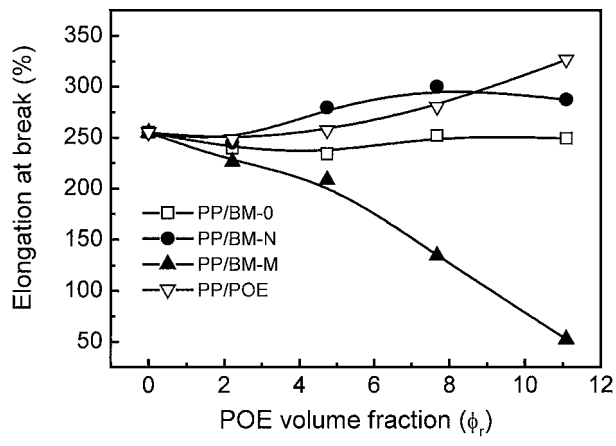

Figure 3 Elongation at break vs. POE volume fraction in PP composites.

owing to the easier deformation of the elastomer. For polymer/elastomer/filler ternary composites, the situations are far more complicated, elongation at break is affected not only by the properties and contents of components, but also by the morphology and interfacial interaction. Strong interfacial interaction could cause the decrease of elongation at break of the composites.

Fig. 4 shows the flexural modulus of PP composites. It is evident that the incorporation of POE elastomer reduced the flexural modulus of PP/POE binary blend significantly, whereas the addition of untreated and coupling agent treated $BaSO_4$ filler increases the modulus of PP ternary composites. In addition, the modulus of the former is higher than that of the latter because the coupling agent would soften PP matrix around filler particles. Contrary results were observed for PP/BM-M ternary composite, whose modulus decreased as yet lower than the modulus of PP/POE binary blend. As shown previously, core-shell morphology exists in PP/BM-M composite, the soft layer of POE elastomer adheres strongly to the surfaces of $BaSO_4$ filler, inhibiting the stiffening action of $BaSO_4$ particles. At the same volume fraction of POE elastomer, the apparent volume fraction of POE elastomer in PP/BM-M composite is larger than that of PP/POE binary composite due to the encapsulation of $BaSO_4$ particles by the POE, resulting in lower modulus in PP/BM-M system.

The notched Izod impact strength of various PP composites was shown in Fig. 5. For PP/POE binary blends, the incorporation of POE elasomer significantly increases the impact strength of PP, a significant increase of impact strength can be observed at the POE concentration between 2.21 and 4.74 vol%, indicating a brittle-tough transition. Further increase of POE concentration causes only slight improvement of the impact strength. The effect of POE concentration on the impact strength of PP/BM-M ternary composite demonstrates similar behavior, except for the relatively lower values. Contrary results were observed for PP/BM-N and PP/BM-0 ternary composites, whose impact strength decreases a little, and then increases when the POE concentration exceeds 4.74 vol%. Within the POE concentration investigated, the impact strength of PP/BM-N composite was slightly higher than that of the PP/BM-0 composite.

The brittle-tough transition in elastomer toughened polymeric systems was reported widely and explained by the percolation model [26]. Previous reports indicate the effect of elastomer on the toughness of PP depends upon the distance between the particles [27, 28]. For PP/elastomer/filler ternary composites, the arrangement of filler in the PP matrix gives rise to the formation of two dissimilar morphologies, i.e., core-shell and separated morphologies. The encapsulation of the filler by the elastomer effectively increases the apparent volume fraction of elastomer, which decreases the distance between the elastomer particles more efficiently than that in composites with separated morphology, resulting in relatively higher impact strength of the former. In addition, the toughening efficiency of elastomer with rigid filler core in ternary composites is expected to be higher as compared with that of the elastomer in binary blends, however, such phenomenon was not observed in the present study. Other researchers [14] also got similar results. The probable explanations are that not all the filler was encapsulated by the elastomer and the elastomer particles with rigid core were not as effective as pure elastomer (Fig. 5).

To investigate the effect of filler particles on the impact strength of ternary composites, relative impact strength is plotted against the $BaSO_4$ volume fraction, shown in Fig. 6. The relative impact strength of PP/BM-M composites is much higher than that of

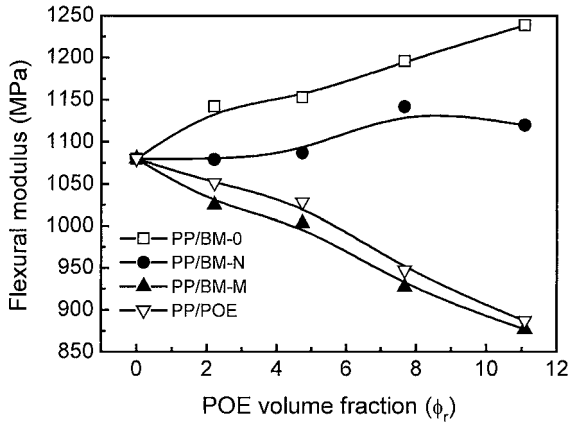

Figure 4 Flexural modulus vs. POE volume fraction in PP composites.

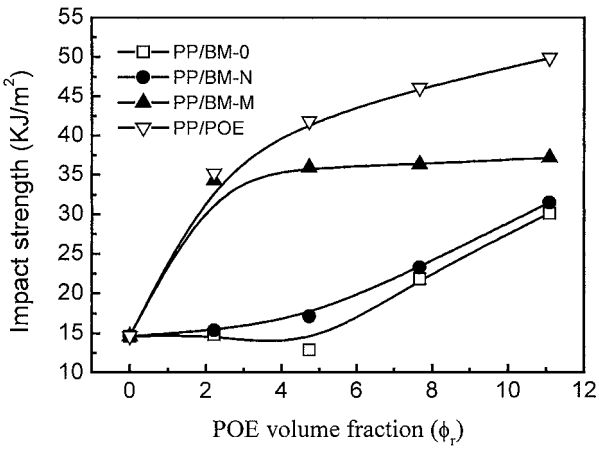

Figure 5 Notched Izod impact strength vs. POE volume fraction in PP composites.

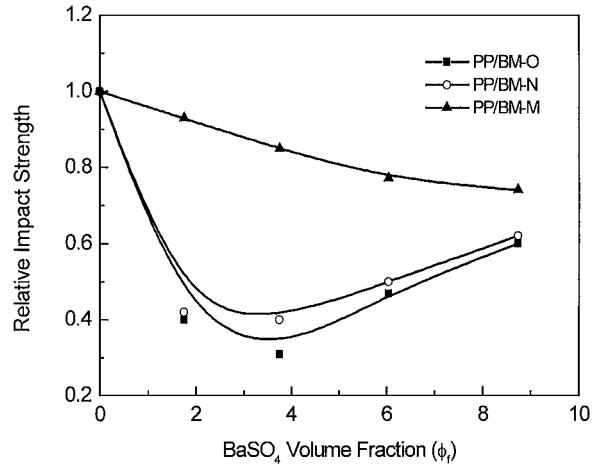

Figure 6 Relative impact strength vs. $BaSO_4$ volume fraction in PP composites.

PP/BM-0 and PP/BM-N composites, indicating that core-shell morphology is benefit to the improvement of impact strength. For PP/BM-M composite with core-shell morphology, the relative impact strength was found to decrease with the increasing of the filler content. Different results were observed for ternary composites with separated morphology, where the relative impact strength passes through a minimum at the filler concentration of 3.75 vol%, then increases with the increase of filler concentration. The relative impact strength of PP/BM-N composite was slightly higher than that of the PP/BM-0 composite, which may be attributed to the poor interfacial interaction between filler particles and PP matrix in the PP/BM-0 composite. The difference in the tendency of the relative impact strength indicates the toughening action of $BaSO_4$ filler in composite with core-shell morphology is inhibited by the elastomer shell, whereas the $BaSO_4$ filler in composites with separated morphologies have significant toughening action when the filler contents exceed 3.75 vol%. Combining Fig. 5 with Fig. 6, it can be found that it is just beyond this point, the combined effect of POE elastomer and $BaSO_4$ particles leads to a synergetic toughening effect on the impact strength of composites with separated morphology.

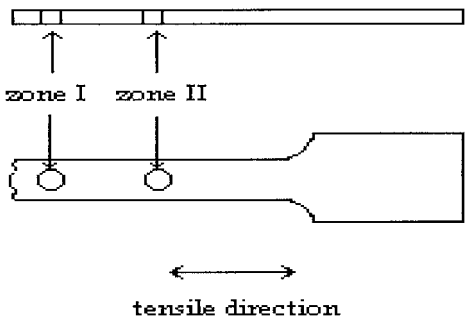

Figure 7 Schematic diagram of longitudinal section of tensile fractured specimen for SEM observation.

3.3. Fracture behavior

In order to investigate the effect of phase structure on the fractured behavior and toughening mechanism of PP/POE/$BaSO_4$ ternary composites, we cut open the tensile fractured surfaces under liquid nitrogen parallel to the tensile direction according to the diagram shown in Fig. 7, and observed the fractured morphology of the longitudinal sections by SEM. Two zones were selected for observation as illustrated in Fig. 7. For the observation of impact fractured surface by SEM, two distinct zones were selected. Zone I is located next to the notch, whereas zone II is in the middle of the fractured surface.

As shown in Figs 8 and 9, in PP/BM-0 composites (Figs 8a and 9a), debonding takes place under tensile loading due to poor adhesion between $BaSO_4$ particles. The debonding action results in the reduction of strain concentration in the PP matrix in the vicinity of the filler particles and matrix [26]. Debonded particles acts as a stress concentrator, which produces micro-cracks along the tensile direction, meanwhile produces a lot of shear yield ribbons perpendicular to the tensile direction to inhibit the formation of continuous cracks. This results in high local strain by the tensile cold drawing and flow of PP matrix. In the zone far from tensile fractured surface (zone II, Fig. 9a), much more shear yield ribbons appear. A lot of ribbons extensively inhibit the propagation of micro-cracks induced by debonded filler particles, indicating a relatively even strain distribution in the matrix. All of these give rise to the high elongation at break and low yield strength.

However, PP/BM-M composites show quite different fractured morphology (Figs 8b and 9b). Core-shell morphology exists and the interaction between $BaSO_4$ filler core and POE elastomer shell is far stronger than that between POE elastomer and PP matrix, and therefore good adhesion exists between the $BaSO_4$ filler and POE. The concentration of strain is high in the vicinity of the core-shell inclusions where the PP matrix deformation is highly restricted. In zone I (Fig. 8b), debonding takes place between the core-shell inclusions and

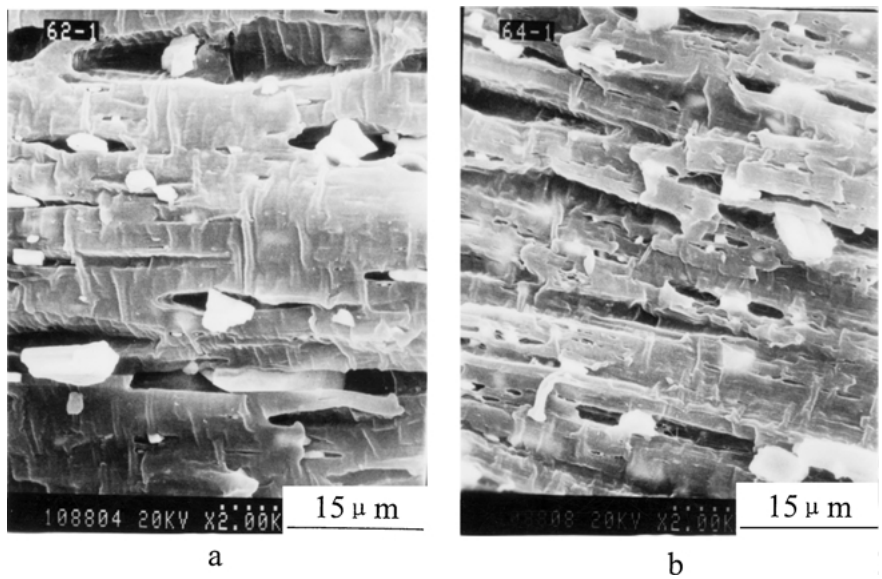

a b

Figure 8 SEM micrographs of longitudinal sections of tensile fractured specimens of PP/POE/$BaSO_4$ composites (zone I) (×2000): (a) PP/BM-0 (60/8/32, by wt) and (b) PP/BM-M (60/8/32, by wt).

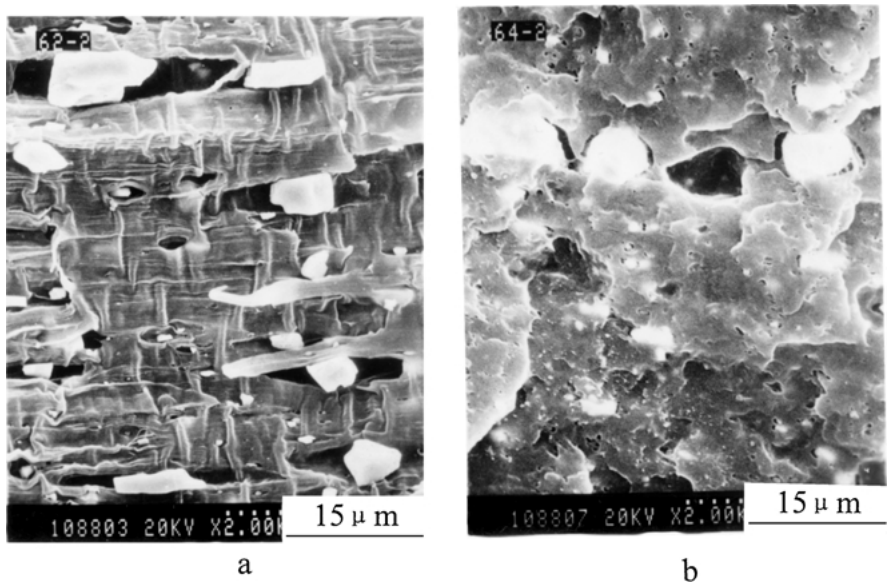

Figure 9 SEM micrographs of longitudinal sections of tensile fractured specimens of PP/POE/$BaSO_4$ composites (zone II) (×2000): (a) PP/BM-0 (60/8/32, by wt) and (b) PP/BM-M (60/8/32, by wt).

the matrix, the deformability of PP matrix is highly constrained due to the reduction of shear yield ribbons. In zone II (Fig. 9b), limited debonding between the core-shell inclusions and the PP matrix is observed, the core-shell inclusions are embedded below the plane of fracture. No cold drawing of the matrix and shear yield ribbons could be observed. This causes the decrease of elongation at break and the increase of yield strength.

Fig. 10 demonstrates SEM micrographs of the impact fractured surfaces of PP/POE binary blend. In zone I (Fig. 10a), certain plastic deformation of PP matrix can be observed, whereas extensive plastic deformation appears in zone II (Fig. 10b), illustrated by the formation of regular striations perpendicular to the direction of crack propagation. Such striations were reported earlier in rubber-toughened polymers [29].

Plastic deformation of the PP matrix and extensive cavitation resulting from debonding of filler particles from PP matrix are the characteristics of the impact fractured surfaces of PP/BM-0 composites with separated morphology, as shown in Fig. 11. The extent of plastic deformation in zone II (Fig. 11b) is larger than that in zone I (Fig. 11a), and no striation perpendicular to the direction of crack propagation can be found.

Fig. 12 demonstrates the characteristics of the impact fractured surfaces of PP/BM-M composite with core-shell morphology. In zone I (Fig. 12a), some holes are visible on the fractured surface, resulting from the partial debonding of core-shell inclusions from PP matrix under impact due to the strong adhesion between the $BaSO_4$ core and the POE shell. PP matrix undergoes plastic deformation. Striations associated with heavily plastically deformed fibrils of the PP matrix are clearly shown in zone II (Fig. 12b). In addition, the core-shell inclusions are destroyed and the POE shells are stretched as filaments that link the $BaSO_4$ particles

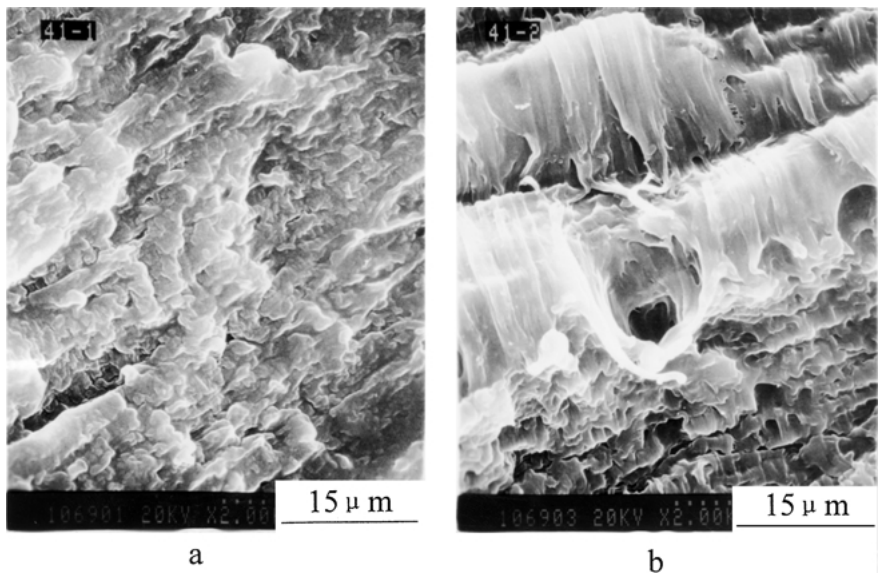

Figure 10 SEM micrographs of impact fractured surfaces of PP/POE (91.3/8.7, by wt): (a) zone I (×2000) and (b) zone II (×2000).

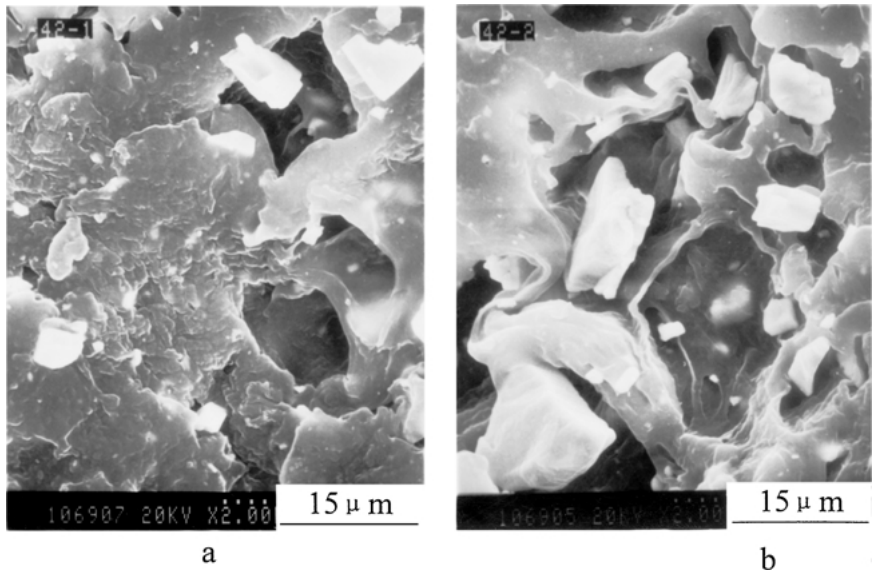

Figure 11 SEM micrographs of impact fractured surfaces of PP/POE/$BaSO_4$ composites (60/8/32, by wt, PP/BM-0): (a) zone I (×2000) and (b) zone II (×2000).

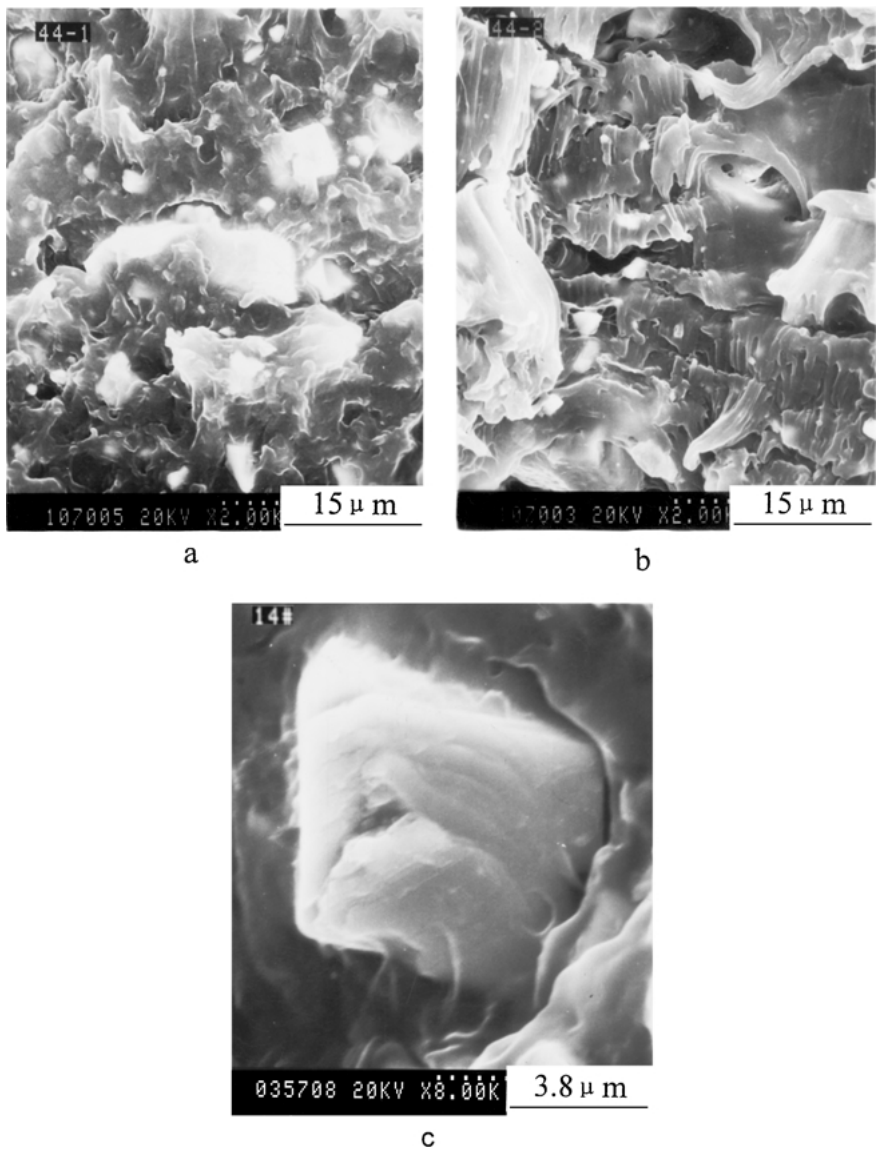

Figure 12 SEM micrographs of impact fractured surfaces of PP/POE/$BaSO_4$ composites (60/8/32, by wt, PP/BM-M): (a) zone I (×2000), (b) zone II (×2000), and (c) zone II (×8000).

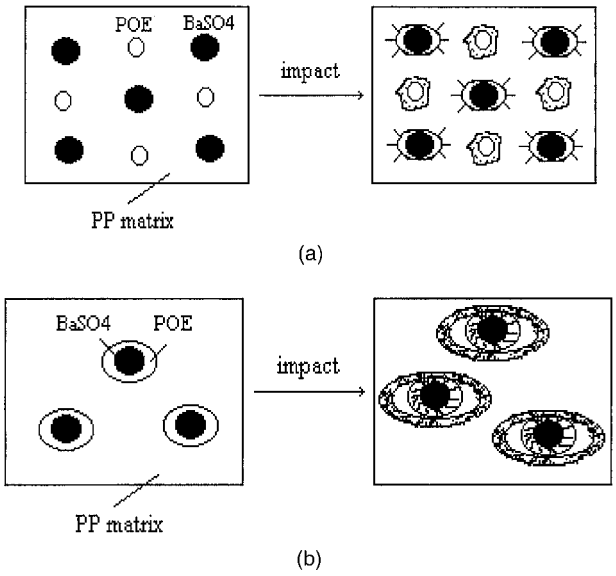

Figure 13 Morphological model of toughening mechanism of PP/POE/$BaSO_4$ ternary composite: (a) separated morphology and (b) core-shell morphology.

with PP matrix. This is believed to be helpful to the enhancement of impact strength and also a crucial factor for the highest impact performance of the PP/BM-M composites. The SEM micrograph at higher magnification (See Fig. 12c) clearly demonstrates this structure.

In view of the above results, we propose two different models of toughening mechanisms for ternary composites with separated and core-shell morphologies, respectively, as shown in Fig. 13. For ternary composite with separated morphology (Fig. 13a), the $BaSO_4$ particles act as stress-concentrator and debond from the PP matrix under impact, producing microcracks. At the same time, shear yielding of PP matrix takes place, which was induced by the POE elastomer, prohibiting the crack propagation to toughen the composites. For the composites with core-shell morphology (Fig. 13b), the core-shell inclusions induce the shear yielding and plastic deformation of the PP matrix under impact stress, meanwhile, the POE shell was peeled off the $BaSO_4$ core, forming filaments that link the $BaSO_4$ particles with the PP matrix, resulting in the destruction of the core-shell inclusions, significantly improving the impact strength of the composites.

4. Conclusions

SEM observation and DSC analysis demonstrate separated morphology exists in ternary composites containing untreated or titanate coupling agent treated $BaSO_4$ particles, where $BaSO_4$ filler promote the crystallization of PP by acting as nucleating agent. Core-shell morphology was obtained in the ternary composites with $BaSO_4$ master-batch prepared by reactive extrusion of POE and $BaSO_4$ in the presence of maleic anhydride and dicumyl peroxide, the nucleating efficiency of $BaSO_4$ filler in PP/BM-M composite was inhibited due to the encapsulation of the filler by POE elastomer.

The mechanical properties of ternary composites were influenced by interfacial interaction and the morphology. The yield strength and the impact strength of a composite with core-shell morphology were higher than those of composites with separated morphology, but the former had lower flexural modulus and elongation at break than the latter. Yield strength was used to quantitatively evaluate the interfacial interaction, indicating the reduction in interfacial interaction because of the titanate coupling agent softening PP matrix around filler particles. Impact strength reveales synergetic toughening effect of POE elastomer and $BaSO_4$ filler on composites with separated morphology when the volume fraction of $BaSO_4$ filler exceedes 3.75 vol%, but the impact strength is still lower than that of composite with core-shell morphology.

SEM observation on impact fractured surface indicates that plastic deformation of the PP matrix and debonding of the filler-matrix are the main toughening mechanisms of composites with separated morphology. For ternary composite with core-shell morphology, in addition to the extensive plastic deformation of the PP matrix, the destruction of core-shell structure was another crucial factor for improving the impact strength.

Acknowledgements

The authors are grateful to the Special Funds for Major State Basic Research Projects of China (G1999064800), National Natural Science Foundation of China and the State Education Ministry of China for financial support of this work.

References

1. B. PUKANSZKY in "Polypropylene: Structure, Blends and Composites," Vol. 3, edited by J. Karger-Kocsis (Chapman & Hall, Composites, London, 1995).
2. R. A. BAKER, L. L. KOLLER and P. E. KUMMER, in "Handbook of Filler for Plastics," 2nd ed, Chap. 6, edited by H. S. Katz and J. V. Milevski (Van Nostrand Reinhold Co., New York, 1987).
3. J. KOLARIK, F. LEDNICKY, J. JANCAR and B. PUKANSZKY, *Polym. Comm.* **31** (1990) 201.
4. W. Y. CHIANG, W. D. YANG and B. PUKANSZKY, *Polym. Eng. Sci.* **32** (1992) 641.
5. B. PUKANSZKY, F. TUDOS, J. KOLARIK and F. LEDNICKY, *Polym. Compos.* **11** (1990) 98.
6. P. R. HORNSBY and K. PREMPHET, *J. Appl. Polym. Sci.* **70** (1998) 587.
7. J. JANCAR, *Macromol. Symp.* **108** (1996) 163.
8. J. KOLARIK, *J. Jancar Polymer* **33** (1992) 4961.
9. K. PREMPHET and P. HORANONT, *J. Appl. Polym. Sci.* **74** (1999) 3445.
10. J. JANCAR and A. T. DIBENEDETTO, *J. Mater. Sci.* **29** (1994) 4651.
11. S. Z. MOLNAR, B. PUKANSZKY, C. O HAMMER and F. H. J. MAURER, *Polymer* **41** (2000) 1529.
12. K. PREMPHET and P. HORANONT, *J. Appl. Polym. Sci.* **76** (2000) 1929.
13. J. JANCAR, A. T. DIBENEDETTO, *J. Mater. Sci.* **30** (1995) 1601.
14. Y. LONG and R. A. SHANKS, *J. Appl. Polym. Sci.* **61** (1996) 1877.
15. Z. BARTCZAK, A. GALESKI, E. MARTUSCELL and H. JANIK, *Polymer* **26** (1985) 1843.
16. E. MARTUSCELL, C. SILVESTRE and G. ALATE, *ibid.* **23** (1982) 229.
17. E. MARTUSCELL, C. SILVESTRE and L. BIANCHI, *ibid.* **24** (1983) 1458.
18. B. PUKANZAKY, F. JUDOS, A. KALLO and G. BODOR, *ibid.* **30** (1989) 1399.
19. F. L. BINSBERGEN, *J. Polym. Sci. Polym. Phys.* **11** (1973) 117.

20. J. KOLARIK, G. L. AGARWAL, Z. KRULIS and J. KOVAR, *Polym Compos* **7** (1986) 463.
21. S. WU, *Polymer* **29** (1985) 2171.
22. B. PUKANSZKY, *New Polym. Mater.* **3** (1992) 205.
23. B. PUKANSZKY, *Composites* **21** (1990) 255.
24. B. TURCSANYI, B. PUKANSZKY and F. TUDOS, *J. Mater. Sci. Lett.* **7** (1988) 160.
25. R. F. GIBSON, in "Principles of Composite Materials Mechanics" (McGraw-Hill, New York, 1994) p. 122.
26. S. H. WU, *Polymer* **26** (1985) 1855.
27. *Idem.*, *J. Polym. Sci. Polym. Phys.* **21** (1983) 699.
28. A. MARGOLINA and S. H. WU, *Polymer* **29** (1988) 2170.
29. O. K. MURATOGLU, A. S. ARGON, R. E. COHEN and M. WEINBERG, *ibid.* **36** (1995) 921.

Received 5 December 2001
and accepted 21 January 2003